



Are the Double-mode Bulge RR Lyrae Stars with Identical Period Ratios the Relic of a Disrupted Stellar System?

Andrea Kunder¹ , Alex Tilton¹, Dylon Maertens¹, Jonathan Ogata¹ , David Nataf² , R. Michael Rich³ ,
Christian I. Johnson⁴ , Christina Gilligan⁵ , and Brian Chaboyer⁵

¹ Saint Martin's University, 5000 Abbey Way SE, Lacey, WA 98503, USA; akunder@stmartin.edu

² Center for Astrophysical Sciences and Department of Physics and Astronomy, The Johns Hopkins University, Baltimore, MD 21218, USA

³ Department of Physics and Astronomy, University of California at Los Angeles, Los Angeles, CA 90095-1562, USA

⁴ Harvard-Smithsonian Center for Astrophysics, Cambridge, MA 02138, USA

⁵ Department of Physics and Astronomy Dartmouth College, Hanover, NH 03784, USA

Received 2019 April 11; revised 2019 May 7; accepted 2019 May 7; published 2019 May 24

Abstract

Radial velocities of 15 double-mode bulge RR Lyrae (RR01) stars are presented, 6 of which belong to a compact group of RR01 stars in pulsation space, with the ratio of first-overtone period to fundamental mode period, $P_{fo}/P_f \sim 0.74$, and $P_f \sim 0.44$. It has been suggested that these pulsationally clumped RR01 stars are a relic of a disrupted dwarf galaxy or stellar cluster, as they also appear to be spatially coherent in a vertical strip across the bulge. However, the radial velocities of the stars presented here, along with proper motions from *Gaia* DR2, show a large range of radial velocities, proper motions, and distances for the bulge RR01 stars in the pulsation clump, much larger than the RR01 stars in the Sagittarius dwarf galaxy (Sgr). Therefore, in contrast to the kinematics of the RRL stars belonging to Sgr, and those in and surrounding the bulge globular cluster NGC 6441, there is no obvious kinematic signature within the pulsationally clumped RR01 stars. If the pulsationally clumped RR01 stars belonged to the same system in the past and were accreted, their accretion in the inner Galaxy was not recent, as the kinematic signature of this group has been lost (i.e., these stars are now well-mixed within the inner Galaxy). We show that the apparent spatial coherence reported for these stars could have been caused by small number statistics. The orbits of the RR01 stars in the inner Galaxy suggest that they are confined to the innermost ~ 4 kpc of the Milky Way.

Key words: Galaxy: bulge – Galaxy: kinematics and dynamics – Galaxy: structure – stars: kinematics and dynamics – stars: Population II – stars: variables: RR Lyrae

1. Introduction

Primordial building blocks are thought to merge and form galaxy bulges (e.g., Abadi et al. 2003; Governato et al. 2007; Brooks & Christensen 2016), and large-scale photometric surveys have revealed many filamentary substructures dubbed stellar streams (e.g., see the “Field of Streams” from Belokurov et al. 2006). Still, no stellar stream has been confirmed as belonging to our Milky Way (MW) bulge. This is in contrast to the many star streams seen in the halo and in the disk (e.g., De Silva et al. 2007; Koposov et al. 2015; Antoja et al. 2018). Many of these streams are thought to be remnants of tidally disrupted systems such as dwarf galaxies or globular clusters, and some are thought to originate from dynamical interactions with the Galactic bar (e.g., Bensby et al. 2007).

One interpretation of the absence of streams belonging to the bulge is that no significant merger events have occurred in the bulge since the epoch of disk formation ($z \sim 3$). This is unexpected within the context of CDM galaxy formation models, but would support claims that the Galaxy has undergone an unusually quiet formation history (e.g., Hammer et al. 2007). Another interpretation is that the signature of a merger in the inner Galaxy just has not been discovered yet. First, the proximity of the bulge (~ 8 kpc) makes it unlikely that streams will be identified from spatial over-densities from photometry (e.g., Helmi et al. 1999). Unfortunately, this is how most of the currently known star streams have been found (see review by Grillmair & Carlin 2016), and where our techniques are most familiar and refined. New approaches and ideas are needed for situations where photometry alone cannot lead to

discoveries. Second, the lifetimes of kinematic substructure in the inner Galaxy will be shorter than that in the halo; an infalling cluster/galaxy will be prone to shorter mixing time-scales in the inner Galaxy due to the more centrally concentrated mass there, resulting in shorter relaxation times (see Section 7.1 Binney & Tremaine 1987). This would suggest that signatures of early debris may already be washed out. However, it has been shown that long-lived streams in the inner Galaxy are still achievable depending on certain conditions, such as if the stream was in resonance with the rotating bar in the inner Galaxy (Hattori et al. 2016). Lastly, the inner Galaxy is a complicated mixture of inner- and outer-disk, inner- and outer-halo, and bulge stars (Robin et al. 2012), where the bulge may also have different and overlapping stellar populations, and disentangling any of these populations, not to mention identifying a new coherent substructure from the inner Galaxy, is daunting.

Still, coherent structures have been seen in the direction of the bulge. Perhaps the most well-known example is the Sagittarius dwarf galaxy (Sgr), discovered as an extended group of stars with common radial velocities in the direction of the Galactic bulge (Ibata et al. 1994). It is our nearest confirmed galactic neighbor, and is a spectacular example of a stellar system caught in the Galaxy’s gravitational pull as being tidally torn apart. More recently, Ophiuchus, the innermost stellar stream known in our Galaxy, was identified (Bernard et al. 2014). It is a thin and long (~ 1.6 kpc) stellar stream that has just passed its pericenter at ~ 3 kpc from the Galactic center (Sesar et al. 2015). Both of these structures are relatively

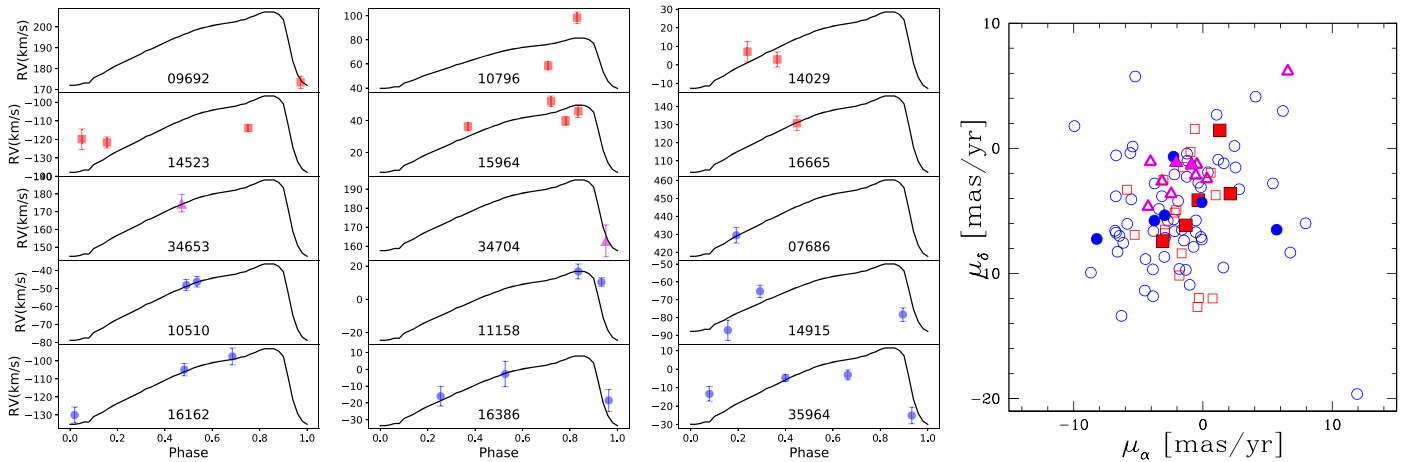


Figure 1. Left: radial velocity curves of observed double-mode RR Lyrae stars. The OGLE-ID for the RR01 stars is also shown. Stars from the grouping in P_{f0}/P_f space are indicated by red squares. Stars from the Sagittarius dwarf galaxy are indicated by magenta triangles. Stars from the galactic bulge not in the P_{f0}/P_f grouping are indicated by blue circles. Right: the *Gaia* DR2 proper motions of double-mode RRLs. Stars for which we have calculated radial velocities are shown as filled symbols, and those without radial velocity information are left open. Note that the Sgr RR01s cluster in proper motion space.

recent debris and so have likely not yet substantially contributed to the current make-up of the Galactic bulge.

One intriguing evidence for substructure in the bulge was presented through the discovery of double-mode RR Lyrae stars in the inner Galaxy. Double-mode RRLs are stars that pulsate simultaneously in both the fundamental and the first-overtone radial pulsation modes, and are known as RRd or RR01 stars. Most often, but not always, it is the first-overtone period (P_{f0}) that has the larger amplitude than the fundamental period (P_f). Curiously, more than 20% of the bulge RR01 stars form a compact group with a ratio of first-overtone period to fundamental mode period of $P_{f0}/P_f \sim 0.74$ and $P_f \sim 0.44$ (see Figure 4, Soszyński et al. 2014, also reproduced here in our Figure 2). Soszyński et al. (2014) therefore suggested that this group of RR01 stars with period ratios around 0.740 form a stream in the sky that may be a relic of a cluster or a dwarf galaxy tidally disrupted by the MW. Not only does the compact nature of this group suggest that these stars belong to the same system, but also no other RR01 stars in the Galaxy have these particular pulsation properties. Furthermore, Soszyński et al. (2014) report that the position of these 28 “pulsationally clumped” groups of RR01 stars in the sky is correlated, in a sense that these stars cross the bulge nearly vertically with only a 1.1% chance that they are drawn from the same general population as the other bulge RRL. Therefore, instead of using photometry or kinematics to disentangle substructure, the strong clumping in pulsation space point to a subset of RR01 stars in the inner Galaxy that appear to have originated from the same stellar structure. Because the spatial distribution of the pulsationally clumped RR01 stars appears to be coherent (Soszyński et al. 2014), this potential debris manifest in pulsation space should be a relatively recent addition to the MW.

Here we explore the dynamics of 15 RR01 stars toward the inner Galaxy that we have obtained radial velocities for with the intent of investigating if the pulsationally clumped RR01 stars are kinematically similar and moving through the Galactic bulge together. With the *Gaia* DR2 data release (Gaia Collaboration et al. 2018), we now have in hand proper motions of the majority of RR01 toward the inner Galaxy with a mean precision of $\sim 5\%$ (note that these stars are too faint for *Gaia* radial velocities or accurate parallaxes).

2. Data

2.1. Radial Velocities

We used the OGLE-III catalog of RRLs (Pietrukowicz et al. 2012) to select RR01 stars that fell within the footprint of the BRAVA-RR survey (Kunder et al. 2016). Therefore, the spectra was taken using the AAOmega multifiber spectrograph on the Anglo-Australian Telescope (AAT) covering the wavelength regime of about 8300–8800 Å at a resolution of $R \sim 10,000$. The observations were taken on four different observing runs: (1) field $(l, b) = (3, -3)$ observed on 2014 June 21—NOAO PropID: 2014A-0143, (2) field $(l, b) = (3, -5)$ observed on 2015 August 19–20—NOAO PropID: 2015B-071, (3) field $(l, b) = (6, -5)$ observed on 2016 August 09–10—2016B-0058, (4) field $(l, b) = (6, -5)$ observed again on 2017 June 18—2017A-0195. Exposure times were between one to two hours, and in general there are one to four epochs for each RR01 star. The reductions were carried out in conjunction with the BRAVA-RR reductions (Kunder et al. 2016).

The radial velocity curves are shown in Figure 1 and presented in Table 1. Table 1 gives the OGLE-ID (1), the R.A. (2) and decl. (3) as provided by OGLE, the star’s time-average velocity (4), the number of epochs used for the star’s time-average velocity (5), the fundamental period of the star (6), the first-overtone period of the star (7), V -band magnitude (8), the I -band magnitude (9) and the I -band amplitude (10) as calculated by OGLE, and lastly the distance adopted for the orbital integration (11).

The RR01 radial velocity measurements have been phased by the stars’ known period, and overplotted with the radial velocity template from Liu (1991). This template is designed for fundamental mode RRL (RR0 pulsators), and the shape is slightly different RR01 stars (as discussed below). The template is scaled using a correlation between the amplitudes of velocity curves and light curves:

$$A_{rv} = \frac{40.5 \times V_{amp} + 42.7}{1.37} \quad (1)$$

as shown in Liu (1991). As in Sesar (2012) and Kunder et al. (2016) we adopt $p = 1.37$, the so-called “projection factor,” to relate our observed radial velocities to the pulsation radial

Table 1
Radial Velocities of Double-mode RR Lyrae Stars

OGLE ID	R.A.	Decl.	HRV $_{\phi = .38}$ (km s $^{-1}$)	# Epochs	Period $_d$ (days)	Period $_{f_0}$ (days)	(V) $_{\text{mag}}$	(I) $_{\text{mag}}$	I_{amp}	Dist(kpc)
09692 ^{ca}	17:59:04.69	-26:59:45.80	191	1	0.44175049	0.32690731	19.475	16.441	0.023	6.8
14029 ^c	18:07:54.91	-29:07:06.60	14	2	0.42994289	0.31798626	16.417	15.399	0.08	6.8
14523 ^c	18:09:07.56	-28:28:49.70	-115	3	0.43271139	0.31999264	17.522	16.122	0.064	9.3
10796 ^c	18:01:01.15	-27:43:43.90	63	2	0.43137749	0.31910024	17.274	15.774	0.07	6.3
15964 ^c	18:14:57.56	-28:01:36.60	31	4	0.43885161	0.32474475	16.08	15.252	0.057	7.7
16665 ^c	18:22:58.23	-25:50:29.30	127	1	0.43427162	0.32112679	16.696	15.575	0.029	7.5
11158	18:01:42.64	-27:58:21.70	-2	2	0.44178959	0.32624505	18.285	16.486	0.273	11.9
07686	17:55:54.44	-36:38:58.50	441	1	0.46652248	0.34684518	16.443	15.377	0.212	8.2
10510	18:00:30.52	-28:26:37.90	-55	2	0.50307068	0.37496547	16.078	14.844	0.114	5.6
14915	18:10:19.99	-28:00:22.50	-67	3	0.43338541	0.31699525	16.496	15.417	0.219	7.1
16162	18:16:15.53	-28:34:36.60	-112	3	0.47774077	0.35538199	16.318	15.553	0.176	10.1
35964	18:18:38.12	-26:04:32.60	-7	4	0.54309504	0.40511131	16.842	15.679	0.1	11.7
16386 ^a	18:18:16.99	-25:12:52.40	-11	3	0.542311	0.40460239	17.296	16.304	0.135	13.6
34653 ^{sgf}	18:12:08.67	-28:57:31.80	169	1	0.47650339	0.35444355	18.966	18.02	0.192	29.7
34704 ^{sgf}	18:12:22.91	-28:49:34.80	178	1	0.47478192	0.35291588	18.297	17.364	0.094	23.0

Notes.

^aNo *Gaia* DR2 proper motion.

^c Period ratio clump.

^{sgf} Sgr dwarf galaxy.

velocities. OGLE samples the I -band much more frequently than the V -band, so we take the OGLE I -amplitude and multiply it by 1.6 to obtain each stars V -amplitude (see, e.g., Table 3 in Kunder et al. 2013).

The main uncertainties in our radial velocity measurements arise from the following factors: (1) We have one to four epochs of observations, so not enough to trace out the full RR01 velocity curve. (2) To compensate for the small number of measurements, we use RR0 light-curve templates to find the center-of-mass velocity, as no RR01 light-curve templates exist in the literature. (3) Our signal-to-noise ratio (S/N) is low, with S/N ~ 5 –20, so our individual radial velocity measurements have uncertainties of ~ 5 km s $^{-1}$. To understand how the first two issues affect our radial velocity measurements, we used the RR01 velocity curves in the globular cluster M3 (Jurcsik et al. 2017, see their Figure 2). We reduced their ~ 100 individual measurements spread out over the full pulsation cycle to only three measurements. We found that the typical error between the data and the measurements using the entirety of the data and the measurements using the decreased data is ~ 5 –15 km s $^{-1}$, depending on what randomly kept three measurements were retained. In particular, stars with observations only on the rising branch (i.e., those between a phase of ~ 0.8 and 1.05) are the most susceptible to large uncertainties. We therefore adopt our radial velocity uncertainty as ~ 15 km s $^{-1}$, which also encompasses the uncertainty in finding individual radial velocity measurements. We note that the stars 09692, 10796, and 34704 likely have the largest radial velocity uncertainties, as our observations for these stars fell on the rising branch of their radial velocity curves.

2.2. Proper Motions

Proper motions of the RR01s are obtained from cross-matching with the *Gaia* DR2 catalog (Gaia Collaboration et al. 2018). We find that 145 of the 173 RR01 stars have a proper motion in the *Gaia* DR2 catalog, where it is mainly the fainter (e.g., the Sgr RR01 stars) that do not have proper motions.

2.3. Distances

To obtain distances to the RR01 stars, first reddenings along the line of sight of each star is obtained from the OGLE bulge extinction maps in Nataf et al. (2013). This extinction map was established using the OGLE-III passbands, similar to the OGLE-IV photometry used here, and makes use of the $E(J - K_s)$ reddening from Gonzalez et al. (2012) to allow the coefficient of selective extinction, R_{JKVI} to vary, which is more realistic in the bulge region. The dereddened color–magnitude diagram is shown in Figure 2. The stars with I_0 greater than ~ 16.7 mag belong to the Sagittarius dwarf galaxy (Sgr). Stars with $I_0 \sim 16$ to ~ 16.7 may also be Sgr stars; however, their proper motions and P_{f_0}/P_f ratio are more consistent with RRLs belonging to the inner Galaxy.

To convert dereddened magnitudes to distances, we use the procedure outlined in Alcock et al. (1997) to calculate luminosities of the RR01 stars. This is based on pulsation equations for model envelopes of RRLs from Bono et al. (1996) and also the assumption that there is a close similarity between the temperature of the blue edge (FBE) of the fundamental instability strip and the transition zone occupied by the multimode stars (Bono & Stellingwerf 1994). Therefore, the period of the fundamental mode at the blue edge of the instability strip can be directly related to a star’s temperature (Sandage 1993a, 1993b) and hence luminosity with the equation

$$\log(L/L_{\odot}) = 2.506 + 2.405 \log P. \quad (2)$$

This equation yields an optical RR01 distance modulus of 18.48 ± 0.19 mag (Alcock et al. 1997) to the LMC, which is one that is consistent with the distance found from eclipsing binaries (Pietrzyński et al. 2013). At $P_0 = 0.46$ days, the approximate period of the bulge RR01 stars in the pulsation clump, $\log L/L_{\odot} = 1.69$. Using an adopted bolometric correction of 0.09 mag (VandenBerg & Bell 1985), this translates to $M_V = +0.49$ for stars at $P_0 = 0.46$ days. This is well within the range of what is found for luminosities of bulge RRLs from other studies (e.g., Lee & Sohee 2016), as well as what is found

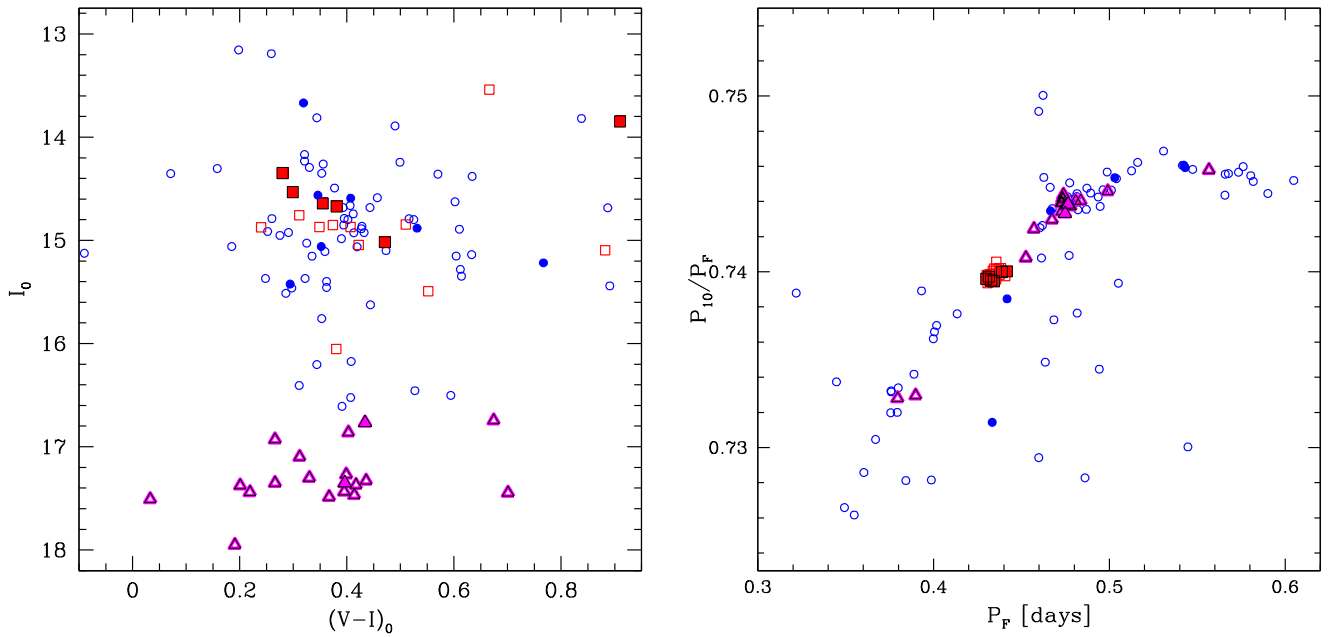


Figure 2. Left: a dereddened color–magnitude diagram of the double-mode RR Lyrae stars for those stars with reddening information from Nataf et al. (2013). Right: the period properties of these bulge RR01 stars. Symbols are as defined in the caption of Figure 1.

for local RRLs with metallicities similar to that of the bulge ($[\text{Fe}/\text{H}] \sim -1.0$ dex) derived from a Baade–Wesselink analysis (Bono et al. 2003; Kovács 2003).

Figure 3 shows how our distances would change if we use the Gonzalez et al. (2012) reddenings and assume an extinction curve from Fitzpatrick (1999).

We also obtained distances following a similar procedure used for bulge RR0 stars in Pietrukowicz et al. (2015), but using newer theoretical absolute magnitude relations for the RRLs (Marconi et al. 2018). Briefly, we first use the mean-flux magnitudes as listed by OGLE-IV. We then find the absolute magnitudes M_V and M_I from the theoretical relations of Marconi et al. (2018):

$$M_V = 0.22[\text{Fe}/\text{H}] - 2.94 \log Y - 1.08 \quad (3)$$

and

$$M_I = 0.471 - 1.132 \log P_f + 0.205 \log Z, \quad (4)$$

where P is the pulsation period as determined by OGLE, $\log Z = [\text{Fe}/\text{H}] - 1.785$, and Y is the helium abundance, which we take as $Y = 0.245$ (Marconi & Minniti 2018). For $[\text{Fe}/\text{H}]$ we use -1.0 dex (Walker & Terndrup 1991). For the pulsation period, because the first overtone period is more accurate than the fundamental mode one, we “fundamentalized” the first overtone period (e.g., van Albada & Baker 1973; Bono et al. 1997; Marconi et al. 2003) using

$$\log P_f = \log P_{f0} + 0.127. \quad (5)$$

The distance can then be found using A_I values from Nataf et al. (2013) and

$$d = 10^{0.2(I_0 - M_I + 5)} \text{ pc}. \quad (6)$$

Our distances can be compared with those found using DR2 parallaxes with a weak distance prior that varies smoothly as a function of Galactic longitude and latitude according to a Galaxy model (Bailer-Jones et al. 2018). All our distances fell within the possible values allowed by the Bailer-Jones et al.

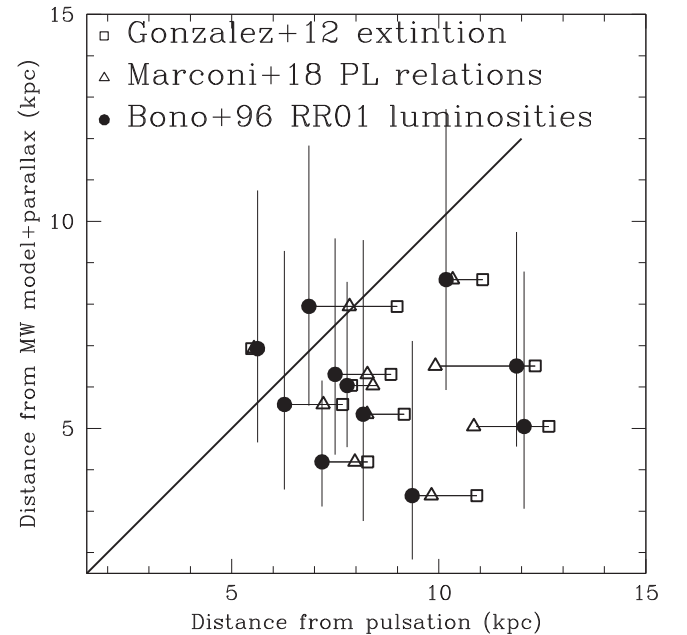


Figure 3. Distances of our observed double-mode RR Lyrae stars obtained from their pulsation properties as compared to distances found using DR2 parallaxes with a weak distance prior that varies smoothly as a function of Galactic longitude and latitude according to a Galaxy model (Bailer-Jones et al. 2018). The closed circles indicate distances found using pulsation equations for RR01 stars from Bono et al. (1996) and reddening values from Nataf et al. (2013). The open triangles indicate distances obtained in the same manner, but with reddening values from Gonzalez et al. (2012) and using the Fitzpatrick (1999) extinction curve. Open squares indicate distances found using new Period–Luminosity–Metallicity–Helium (PLZY) relations from Marconi et al. (2018) and reddening values from Nataf et al. (2013). Different pulsation equations and reddening values lead to distance uncertainties of ~ 1 kpc.

(2018) error margins with the exception of three stars, 14523, 11158, and 16162. The distances from Bailer-Jones et al. (2018) assumes the RRLs peak at a distance of ~ 6 kpc instead of ~ 8 kpc, which is the distance of the bulge (Bland-Hawthorn & Gerhard 2016). This shorter distance is unlikely, as these are

RRLs in the direction of the bulge with a magnitude distribution consistent with them being located in the inner Galaxy (see Figure 2). In contrast, the distances using RR01 pulsation properties peak at ~ 8 kpc, in agreement with other distances of the RRL population toward the inner Galaxy (e.g., Dékány et al. 2013).

2.4. Orbital Information

Combining R.A. (α) and decl. (δ) positions, distances, proper motions in α and δ , and radial velocities, Galactocentric spherical polar components of the velocities (radial v_r , azimuthal v_θ) for our RR01s were calculated. We adopted left-handed Galactic Cartesian coordinates, so that the x -axis (i.e., U velocity) is positive going away from the Galactic center, the y -axis (i.e., V velocity) is positive in the direction of Galactic rotation, and the z -axis (i.e., W velocity) is positive toward the North Galactic Pole (NGP). The local standard of rest is $v_{\text{LSR}} = 220 \text{ km s}^{-1}$ (e.g., Bovy et al. 2012), and the distance to the Galactic center adopted is 8.2 kpc (Bland-Hawthorn & Gerhard 2016). Orbital information is calculated using the `galpy` Python package,⁶ where the potential adopted is the recommended MW-like potential `MWPotential2014` (Bovy 2015).

3. Discussion

Unlike the RR0 stars (fundamental mode RRL), the RR01 variables are rare in the bulge of our Galaxy (this is especially evident in the OGLE-IV catalog presented in Soszyński et al. 2014). This is also the case for RR01 stars in Galactic globular clusters and in the field (e.g., Clement et al. 2001; Szczygiel & Fabrycky 2007). They are instead more frequent in the field of other Local Group dwarf galaxies, where new surveys using wide-field detectors and continuous monitoring are constantly increasing their number (e.g., Kovács 2001; Dall’Ora et al. 2006; Kinemuchi et al. 2008; Coppola et al. 2015). For example, only $\sim 0.5\%$ of the OGLE bulge RRL are RR01 stars (Soszyński et al. 2014), whereas there is a $\sim 5\%$ incidence rate of RR01 stars in the OGLE LMC sample, and more than 10% of RRL are double-mode pulsators in the OGLE SMC sample (Soszyński et al. 2016).

With the exception of the bulge, all systems with double-mode pulsators are metal-poor (with $[\text{Fe}/\text{H}] < -1.5$ dex), and all show a ranking in a sense that the P_{f0}/P_f ratio becomes smaller in more metal-rich systems. For the bulge, the small RR01 period ratios indicate an extended metal-rich component that no other region in the Galaxy (or dwarf galaxy) harbors. Hence, these objects offer a unique way to trace properties of an old regime that is not possible in the halo. (Note that the metal-rich globular clusters in the Galaxy in which RRL reside, NGC 6441 and NGC 6338, do not have RR01 stars; see the Catalogue of Variable Stars in Galactic Globular Clusters in Clement et al. 2001).

Masses of RR01 pulsators are evaluated from the ratio between the first overtone (P_{f0}), and the fundamental (P_f) pulsation periods and pulsation models trace loci of constant mass in a diagram that plots the P_{f0}/P_f ratio versus P_f , from which stellar masses can be estimated (Bono et al. 1996). Therefore, they provide an estimate of the mass and the mass–metallicity relation of horizontal branch stars. The similarity in

P_{f0}/P_f and P_f of the pulsationally clumped RR01s indicate that they have little spread in masses and chemistry, further suggestive that these stars belong to a unique system.

Radial velocities of 15 double-mode RR Lyrae stars are calculated and presented in Table 1 and Figure 1. Six of these belong to the clump in P_{f0}/P_f period space. The radial velocities of these six RR01 pulsationally clumped stars span a wide range of values, covering a range of $\sim 300 \text{ km s}^{-1}$. Two groups of two RR01 stars are spatially closer to each other than the other RR01s in our sample. First, 10796 and 10510 are $0^\circ 72'$ apart, with $(l, b) = (2.7607, -2.3070)$ and $(l, b) = (2.0830, -2.5628)$, respectively. They have radial velocities, however, that span a large range, with 63 km s^{-1} and -51 km s^{-1} , respectively. Second, 14029 and 14523 are $0^\circ 69'$ apart, with $(l, b) = (2.2868, -4.3085)$ and $(l, b) = (2.9757, -4.2343)$, respectively. They also have radial velocities that span a large range, with 14 km s^{-1} and -115 km s^{-1} , respectively. Although disrupted clusters should show some radial velocity dispersion, especially if spread over degrees over the sky, such a large radial velocity spread between stars within $\sim 1^\circ$ spatial proximity is not expected nor seen from other recent accretion events (e.g., Anguiano et al. 2016; Huang et al. 2019).

Furthermore, the proper motions of all pulsationally clumped RR01 stars span almost the full range of proper motion space, and there is clearly no correlation in the proper motions of the stars with similar period ratios P_{f0}/P_f (Figure 1). This is in contrast to the Sgr stars, that have similar proper motions and radial velocities, as well as a clumping of RR01s with period ratios of $P_{f0}/P_f = 0.744$ and $P_f = 0.47$ days (see Figure 2).

All three components of velocity for the pulsationally clumped RR01s indicate that they are not a coherent moving group. The spatial coherence observed by Soszyński et al. (2014) may be due to small number statistics, as the sample size of the pulsationally clumped RR01 stars in OGLE-IV is 28. The Kolmogorov–Smirnov (K-S) goodness-of-fit test used by Soszyński et al. (2014) requires a sufficient sample size, where $n > 50$ is a good rule of thumb (e.g., Fasano & Franceschini 1987). We also have performed a two-dimensional K-S test to establish whether one can reject the null hypothesis that the two samples of RR01 Galactic latitudes and longitudes (pulsationally clumped RR01s and regular bulge RR01s) come from the same distribution. The K-S test returns a probability of $P = 0.038$, below the default threshold $P_{\text{th}} = 0.05$ below which one rejects the null hypothesis. On this basis, as the OGLE team first reported, it could be assumed that the spatial distribution of the pulsationally clumped RR01s and the regular bulge RR01s are not drawn from the same sample.

To test how the small sample size affects the K-S test, we removed one star from the sample of 28 pulsationally clumped RR01 stars and recalculated the P -statistic. The removed star was then reinserted in the sample, and the next star was removed in an iterative manner. Figure 4 shows how the P -statistic varies if one pulsationally clumped RR01 star is removed from the sample. We see that the P -statistic does have a noticeable effect on the exact value of the P -statistic of a KS-test when using this small sample of stars. Therefore, it is unclear from the KS-test alone if the pulsationally clumped RR01s are a spatially coherent structure extending across the bulge.

⁶ <http://github.com/jobovy/galpy>; version 1.2.

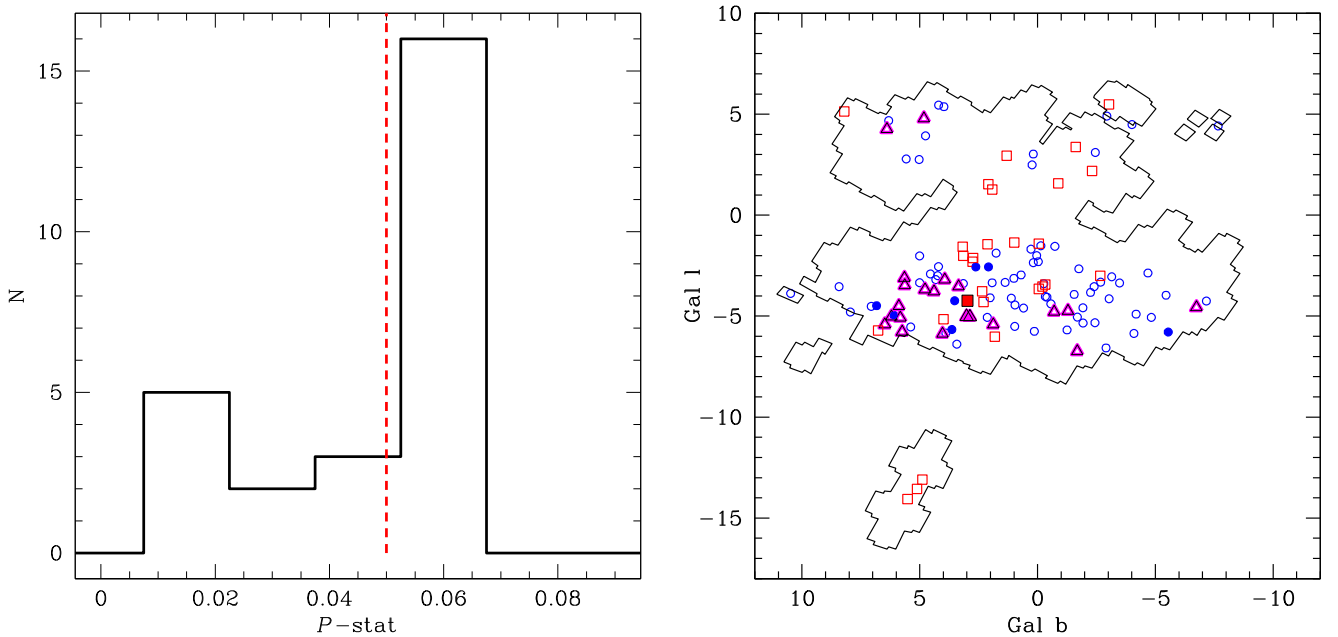


Figure 4. Left: we ran a two-dimensional K-S test to establish whether one can reject the null hypothesis that the pulsationally clumped sample of RR01 stars and the regular RR01 stars come from the same distribution in Galactic latitude and longitude space. This histogram shows the spread in P -statistic values from the K-S test if one pulsationally clumped RR01 star is removed from the sample. The small sample of pulsationally clumped RR01 stars makes it difficult to discern if the P -statistic is above the default threshold $P_{\text{th}} = 0.05$ below which one rejects the null hypothesis. Right: the spatial location in Galactic coordinates (in degrees) of the double-mode RRLs shown in Figure 2; symbols are also defined there. The Galactic center is at $(l, b) = (0, 0)$, and the closed regions show the OGLE-IV search areas.

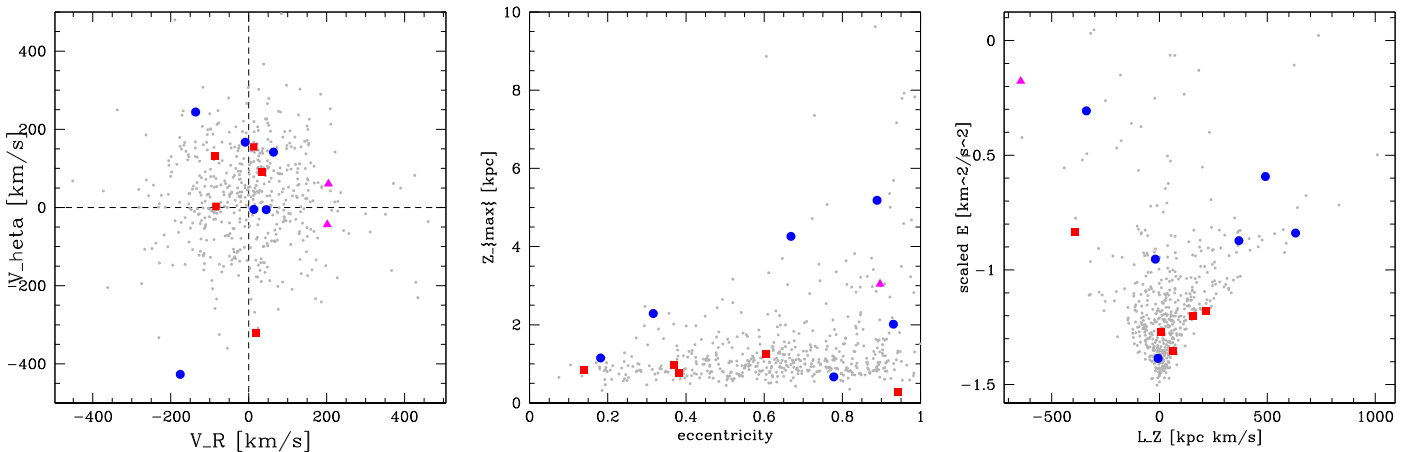


Figure 5. Left: behavior of the velocity components in spherical polar coordinates, namely radial v_r , and azimuthal v_θ , for the RR01 stars presented here. The symbols are the same as those in Figure 1. The bulge RRLs from Kunder et al. (2016) are shown in gray. Middle: the eccentricity and Z_{max} distance of our RR01 stars. Right: the distribution of total Energy and z -angular momentum, L_z , where L_z is the angular momentum out of the plane of the Galaxy’s disk. The total Energy is divided by 10^5 .

Also, although the main body of the bulge is observed to be relatively symmetrical, the OGLE fields extend to $b \sim 15^\circ$ on only one side of the bulge, so as to observe the main body of the Sgr Galaxy. Three pulsationally clumped RR01 stars are found in the main body of Sgr, which just happens to be located along the proposed nearly vertical direction of the RR01 “stream.” However, no OGLE fields are observed on the other side of the bulge. Therefore, this vertical “alignment” may be due to the fact that RR01 stars were not able to be discovered in the other directions compared to the main body of the bulge.

Figure 5 shows the spherical polar components of the velocities (radial v_r , and azimuthal/tangential v_θ) of the RR01 stars presented here overplotted on the RRLs from Kunder et al. (2016). There is no obvious similarity in these velocities.

The pulsationally clumped RR01s also show a wide range of eccentricities, Z_{max} distances, angular momentum, and energies. The uncertainties on our orbital parameters are considerable—in some cases, greater than 100% due mainly to the distance and radial velocity uncertainties of the RR01 stars (see, e.g., Figure 3). However, the general trends of the distribution of the orbital parameters remain; the pulsationally clumped RR01s, even within their respective uncertainties, do not form any discernible orbital similarities.

We cannot rule out that within the pulsationally clumped RR01s, a subset belongs to a moving group. For example, 14029 and 15964 have radial velocities within 1σ of each other, and similar proper motions. They are spatially $\sim 2^\circ$ apart from each other. A larger sample of RR01s with radial velocities, radial velocity estimates with smaller uncertainties, and

detailed abundance information could give more insight on moving groups within the pulsationally clumped bulge RR01s.

In general, the bulge RR01 stars have apocenter distances less than ~ 4 kpc. The exception is 07686 (the RR01 star with a radial velocity of $\sim 441 \text{ km s}^{-1}$) and the Sgr RR01 stars. This indicates that most of the RR01 stars are confined to the inner Galaxy, but that roughly $\sim 15\%$ are halo outliers just passing through the bulge (see also Kunder et al. 2015).






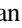

4. Conclusion

The RR01 stars belonging to a compact group of RR01 stars in pulsation space, with period ratios of $P_{f0}/P_f \sim 0.74$ and $P_f \sim 0.44$, possess a large range of radial velocities and proper motions, and are therefore not all moving together in a coherent structure. This is in contrast to the suggestion that these 28 stars are associated with a stellar stream that nearly vertically crosses the bulge, similar to the tidal stream of the Sgr Galaxy (Soszyński et al. 2014). Spatial coherence would indicate that these stars were remnants of a relatively recent merger (like the Sgr merger), as the positional signature of the stars is still intact, and hence that some kinematic signature would be retained.

Although we find that the Sgr RR01 stars have similar radial velocities, proper motions, and period ratios, this is not the case for the pulsationally clumped RR01s, whose radial velocities span $\sim 300 \text{ km s}^{-1}$ and whose proper motions span 12 mas yr^{-1} . Most of the bulge RR01 stars have orbits that confine them to the inner ~ 4 kpc of the Galaxy, but we are not able to find any coherence in the pulsationally clumped RR01s and 3D velocities, angular momentum, or orbital parameters. If the pulsationally clumped RR01s are indeed the relic of a stellar cluster or a dwarf galaxy disrupted by tidal interactions with the MW, any kinematic signature has now been lost.

We thank the Australian Astronomical Observatory, which made these observations possible. The grant support provided, in part, by the M.J. Mudrock Charitable Trust (NS-2017321) is acknowledged.

ORCID iDs

Andrea Kunder  <https://orcid.org/0000-0002-2808-1370>
Jonathan Ogata  <https://orcid.org/0000-0002-8082-7395>
David Nataf  <https://orcid.org/0000-0001-5825-4431>
R. Michael Rich  <https://orcid.org/0000-0003-0427-8387>
Christian I. Johnson  <https://orcid.org/0000-0002-8878-3315>
Christina Gilligan  <https://orcid.org/0000-0003-4510-0964>
Brian Chaboyer  <https://orcid.org/0000-0003-3096-4161>

References

- Abadi, M. G., Navarro, J. F., Steinmetz, M., & Eke, V. R. 2003, *ApJ*, 591, 499
Alcock, C., Allsman, R. A., Alves, D., et al. 1997, *ApJ*, 482, 89
Anguiano, B., De Silva, G. M., Freeman, K., et al. 2016, *MNRAS*, 457, 2078
Antoja, T., Helmi, A., Romero-Gomez, M., et al. 2018, *Natur*, 561, 360
Bailer-Jones, C. A. L., Rybizki, J., Fouesneau, M., Mantelet, G., & Andrae, R. 2018, *AJ*, 156, 58
Belokurov, V., Zucker, D. B., Evans, N. W., et al. 2006, *ApJL*, 642, 137
Bensby, T., Oey, M. S., Feltzing, S., & Gustafsson, B. 2007, *ApJL*, 655, L89
Bernard, E. J., Ferguson, A. M. N., Schlafly, E. F., et al. 2014, *MNRAS*, 443, 84
Binney, J., & Tremaine, S. 1987, *Galactic Dynamics* (Princeton, NJ: Princeton Univ. Press)
Bland-Hawthorn, J., & Gerhard, O. 2016, *ARA&A*, 54, 529
Bono, G., Caputo, F., Castellani, V., et al. 2003, *MNRAS*, 344, 1097
Bono, G., Caputo, F., Castellani, V., & Marconi, M. 1996, *ApJL*, 471, 33
Bono, G., Caputo, F., Castellani, V., & Marconi, M. 1997, *A&AS*, 121, 327
Bono, G., & Stellingwerf, R. F. 1994, *ApJS*, 93, 223
Bovy, J. 2015, *ApJS*, 216, 29
Bovy, J., Allende Prieto, C., Beers, T. C., et al. 2012, *ApJ*, 759, 131
Brooks, A., & Christensen, C. 2016, *ASSL*, 418, 317
Clement, C. M., Muzzin, A., Dufton, Q., et al. 2001, *AJ*, 121, 2587
Coppola, G., Marconi, M., & Stetson, P. B. 2015, *ApJ*, 814, 71
Dall’Ora, M., Clementini, G., Kinemuchi, K., et al. 2006, *ApJL*, 653, L109
Dékány, I., Minniti, D., Catelan, M., et al. 2013, *ApJL*, 776, L19
De Silva, G. M., Freeman, K. C., Bland-Hawthorn, J., Asplund, M., & Bessel, M. S. 2007, *AJ*, 133, 694
Fasano, G., & Franceschini, A. 1987, *MNRAS*, 225, 155
Fitzpatrick, E. L. 1999, *PASP*, 111, 63
Gaia Collaboration, Brown, A. G. A., Vallenari, A., et al. 2018, *A&A*, 616, A1
Gonzalez, O. A., Rejkuba, M., Zoccali, M., et al. 2012, *A&A*, 543, 13
Governato, F., Willman, B., Mayer, L., et al. 2007, *MNRAS*, 374, 1479
Grillmair, C. J., & Carlin, J. L. 2016, *ASSL*, 420, 87
Hammer, F., Puech, M., Chemin, L., Flores, H., & Lehnert, M. D. 2007, *ApJ*, 662, 322
Hattori, K., Erkal, D., & Sanders, J. L. 2016, *MNRAS*, 460, 497
Helmi, A., White, S. D., de Zeeuw, P. T., & Zhao, H. 1999, *Natur*, 402, 53
Huang, Y., Liu, X., Chen, B., et al. 2019, 2018 arXiv:180603748H
Ibata, R. A., Gilmore, G., & Irwin, M. J. 1994, *Natur*, 370, 194
Jurcsik, J., Smitola, P., Hajdu, G., et al. 2017, *MNRAS*, 468, 1317
Kinemuchi, K., Harris, H. C., Smith, H. A., et al. 2008, *AJ*, 136, 1921
Koposov, S. E., Belokurov, V., Torrealba, G., & Evans, N. W. 2015, *ApJ*, 805, 130
Kovács, G. 2001, *A&A*, 375, 469
Kovács, G. 2003, *MNRAS*, 342, 58
Kunder, A., Rich, R. M., Hawkins, K., et al. 2015, *ApJ*, 808, 12
Kunder, A., Rich, R. M., Koch, A., et al. 2016, *ApJ*, 821, 25
Kunder, A., Stetson, P., Cassisi, S., et al. 2013, *AJ*, 146, 119
Lee, Y.-W., & Sohee, J. 2016, *ApJ*, 833, 236
Liu, T. 1991, *PASP*, 103, 205
Marconi, M., Bono, G., Pietrinfermi, A., et al. 2018, *ApJ*, 864, 13
Marconi, M., Caputo, F., Di Criscienzo, M., & Castellani, M. 2003, *ApJ*, 596, 299
Marconi, M., & Minniti, D. 2018, *ApJ*, 853, 20
Nataf, D. M., Gould, A., Fouqué, P., et al. 2013, *ApJ*, 769, 88
Pietrukowicz, P., Kozłowski, S., Skowron, J., et al. 2015, *ApJ*, 811, 113
Pietrukowicz, P., Udalski, A., Soszyński, I., et al. 2012, *ApJ*, 750, 169
Pietrzyński, G., Graczyk, D., Gieren, W., et al. 2013, *Natur*, 495, 76
Robin, A. C., Marshall, D. J., Schultheis, M., & Reylé, C. 2012, *A&A*, 538, 106
Sandage, A. R. 1993a, *AJ*, 106, 687
Sandage, A. R. 1993b, *AJ*, 106, 703
Sesar, B. 2012, *AJ*, 144, 114
Sesar, B., Bovy, J., Bernard, E. J., et al. 2015, *ApJ*, 809, 59
Soszyński, I., Udalski, A., Szymański, M. K., et al. 2014, *AcA*, 64, 177
Soszyński, I., Udalski, A., Szymański, M. K., et al. 2016, *AcA*, 66, 131
Szczygiel, D. M., & Fabrycky, D. C. 2007, *MNRAS*, 377, 1263
van Albada, T. S., & Baker, N. 1973, *ApJ*, 185, 447
VandenBerg, D. A., & Bell, R. A. 1985, *ApJS*, 58, 561
Walker, A. R., & Terndrup, D. M. 1991, *ApJ*, 378, 119